Single-photon core-valence double ionization of molecular oxygen

E. Andersson,[1] M. Stenrup,[2] J. H. D. Eland,[3] L. Hedin,[1] M. Berglund,[1] L. Karlsson,[1] Å. Larson,[2,4] H. Ågren,[2]
J.-E. Rubensson,[1,5] and R. Feifel[1]
[1]*Department of Physics and Material Sciences, Uppsala University, Box 530, SE-751 21 Uppsala, Sweden*
[2]*Department of Theoretical Chemistry, School of Biotechnology, Royal Institute of Technology, SE-106 91 Stockholm, Sweden*
[3]*Physical and Theoretical Chemistry Laboratory, Oxford University, South Parks Road, Oxford OX1 3QZ, United Kingdom*
[4]*Department of Physics, Stockholm University, AlbaNova University Centre, SE-106 91 Stockholm, Sweden*
[5]*BESSY, Albert-Einstein-Strasse 15, D-12489 Berlin, Germany*
(Received 4 July 2008; published 18 August 2008)

Single-photon core-valence double ionization of molecular oxygen has been studied using a magnetic bottle time-of-flight electron coincidence spectrometer. The $K^{-1}V^{-1}$ double ionization electron spectrum of O_2 is reported and is assigned with the aid of *ab initio* calculations. A direct comparison of the core-valence double ionization electron spectra with the conventional valence band photoelectron spectrum is made. The lowest core-valence double ionization energy is found to be 571.6 eV and is associated with a $^3\Pi$ dicationic state.

DOI: 10.1103/PhysRevA.78.023409 PACS number(s): 33.80.Eh, 33.70.Ca, 34.50.Gb

I. INTRODUCTION

Single-photon double ionization electron spectroscopy of atoms and molecules has become a growing field of research due to the advent of a highly efficient and versatile multi-electron coincidence technique [1,2] based on a magnetic bottle [3]. By plotting intensity versus correlated electron pair energy sums, this technique reveals complete double ionization electron spectra, directly analogous to conventional photoelectron spectra, with unprecedented ease and good energy resolution. It gives also deeper insights into the underlying double ionization mechanisms. Whereas previous investigations using this technique have focused mainly on the removal of two valence electrons (see e.g., Refs. [1,4–10]), only a few studies so far involve core electrons [11,12].

The electronic structure of the oxygen molecule has been extensively studied using XPS (x-ray photoelectron spectroscopy), UPS (ultraviolet PS), and Auger methods. XPS and UPS have provided detailed information about the electronic states of the cation, while Auger electron spectroscopy (AES) has revealed energies for dicationic states associated with double valence vacancies. References to numerous works in these fields can be found in Refs. [13] (XPS), [14] (UPS), and [15,16] (AES). Detailed studies of the dicationic valence states of O_2 have also been performed both with the threshold photoelectrons coincidence (TPESCO) [17] and the present time-of-flight photoelectron-photoelectron coincidence (TOF-PEPECO) [8] spectroscopy techniques.

In this work, we present an investigation of core-valence double ionization of molecular oxygen where one of the two electrons is removed from the O 1*s* shell and the other from the valence shell. Spectra were recorded at several photon energies and provide the measurements of core-valence double hole state energies in O_2. Assignments are made with the aid of *ab initio* calculations and by comparison with the conventional valence band photoelectron spectrum.

II. EXPERIMENTAL DETAILS

We have used a 2.2 m magnetic bottle time-of-flight electron coincidence spectrometer described in more detail in Ref. [18], where several electrons can be detected in coincidence and resolved in energy [1,2]. This instrument makes it possible to detect kinetic energies ranging from zero to hundreds of eVs, at an optimal resolution of tens of meV at the lowest kinetic energies and at a nearly constant numerical resolution of about 50 at high kinetic energies. The magnetic bottle design allows detection of electrons emitted over essentially the whole solid angle.

The experiments were performed at the soft-x-ray undulator beamlines U49/2 PGM1 [19] and U49/2 PGM2 [20] at BESSY-II in Berlin, Germany, using photon energies in the range ~600–650 eV. The monochromator bandwidth was set to around 300 meV for these measurements. Single-bunch operation of the storage ring provided 30 ps light pulses with a 800.5 ns period between the pulses [21].

The start of the coincidence measurements is triggered in these experiments by the arrival of the fast, first electron, which is referenced to the ionizing ring pulse. Calibration of the time-to-energy conversion was done by measuring photoelectron and Auger lines of molecular oxygen of known energies [13,15] and by using well-known autoionization lines of atomic oxygen [22] as inherent calibrant. The time-to-energy conversion gave consistent results for the recordings at the first two photon energies, 605 and 620 eV, whereas in the 650 eV recording we encountered line shifts of almost 1 eV, which were most probably due to a decreasing accuracy of the applied time-to-energy equation at higher electron kinetic energies. O_2 gas was commercially obtained with a stated purity of >99.95%.

III. THEORETICAL DETAILS

The electronic structure calculations have been carried out with the Dalton 2.0 program package [23] using a multiconfiguration self-consistent-field (MCSCF) type of wave function and the augmented correlation-consistent polarized valence quadruple zeta (aug-cc-pVQZ) basis set [24,25]. To facilitate further discussion we remind the reader that the leading electron configuration of the $X\,^3\Sigma_g^-$ ground state of neutral molecular oxygen can be written as

$$(1\sigma_g)^2(1\sigma_u)^2(2\sigma_g)^2(2\sigma_u)^2(3\sigma_g)^2(1\pi_u)^4(1\pi_g)^2.$$

Core ionization of symmetric species poses a dilemma which has been extensively dealt with in the literature since the first Delta SCF calculations of core hole states became available. In fact, molecular oxygen was the first system used to demonstrate this dilemma [26]. Unlike symmetric polyatomic species, where symmetric core hole states are subject to quasi-Jahn-Teller interaction and a physical lowering of the point group symmetry, diatomics have no antisymmetric modes available to effect a symmetry lowering. Although symmetry must be retained, the symmetry adapted solutions in the one-particle (SCF) picture suffers from large errors giving ionization energies that are typically more than 10 eV off. On breaking the symmetry, this error is reduced to the magnitude of normal errors from Delta SCF calculations, typically 1 eV for *K*-shell electrons. It is clear that the relaxation energy described in the symmetry broken solution transforms to an electron correlation effect in the symmetry adapted calculation [27]. In molecular oxygen it turns out that the inclusion of both $1\sigma_g$ and $1\sigma_u$ core hole configurations within the same expansion captures a significant part of this correlation, but still not the major portion [27]. In the present work we make use of the fact that modern MCSCF techniques allow sufficiently large active spaces to capture the major part of the electron correlation, and therefore allow all calculations to be conducted in the correct point group symmetry, something which also considerably eases interpretation of the spectra. In the full configuration interaction (CI) picture, symmetry broken and symmetry adapted solutions provide the same result.

The present expansion of the core-valence hole states was generated from a partitioning of the orbital space into two restrictive active spaces (RAS). The RAS1 space was constructed from the $1\sigma_g$ and $1\sigma_u$ orbitals and was restricted to have a permanent occupancy of three electrons. The RAS2 space was constructed from the (2-4)σ_g, (2-3)σ_u, (1-2)π_u, and (1-2)π_g orbitals. Within this subspace all possible distributions of the remaining 11 electrons were allowed. To prevent any variational collapse of the wave function, the orbitals in RAS1 were kept frozen during the optimization. The relaxation energy, i.e., the energy contribution coming from the relaxation of the RAS1 orbitals, was calculated for the lowest core-valence hole state and was then taken as common to all the other states.

In order to obtain the double ionization energies, a calculation on the ground state of the neutral molecule using the same method and basis set was also performed. Here, the $1\sigma_g$ and $1\sigma_u$ orbitals were kept fully occupied and inactive while the remaining 12 electrons were distributed in all possible ways among the RAS2 orbitals defined above. Both the neutral ground state and the core-valence hole states were optimized at the experimentally determined O_2 bond length of 1.20748 Å [28].

IV. RESULTS AND DISCUSSION

Figure 1 shows the core-valence double ionization electron spectra recorded at three different photon energies, 605 eV, 620 eV, and 650 eV, drawn on the same ionization energy scale. The spectra show several bandlike, well-defined structures covering the range between approximately 570 eV and 600 eV. Within the experimental accuracy we do not find any excitation-energy dependence in the investigated energy range. The energy sharing between the two electrons also suggests that the final states are populated primarily in a direct process. The underlying, unstructured intensity reflects partly real coincidences that correspond to doubly ionized states but partly also accidental coincidences of electrons arising from different processes. The double ionization spectrum begins with the strong line at 571.6 eV.

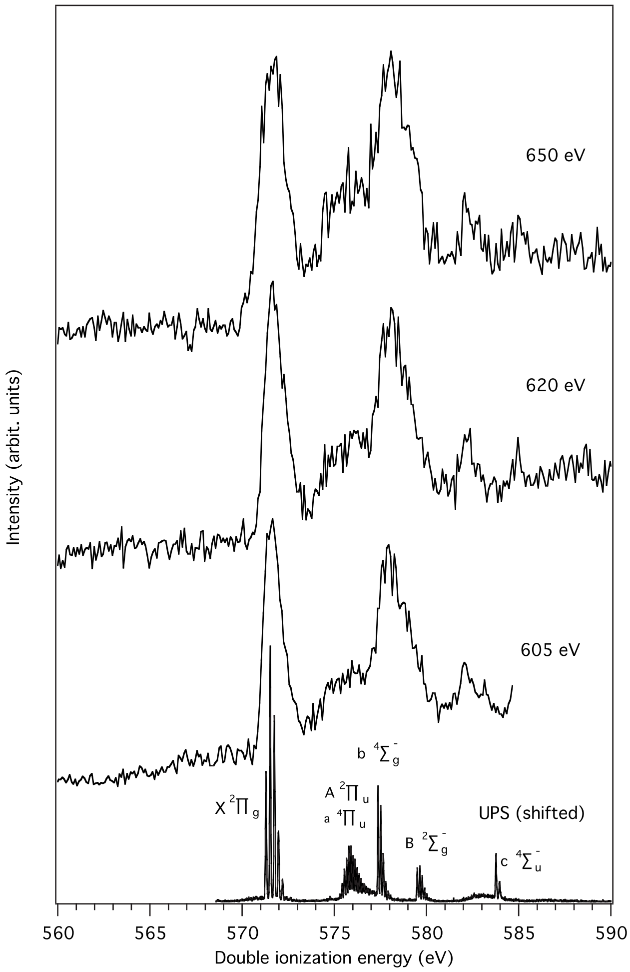

FIG. 1. Core-valence double ionization spectra of the oxygen molecule recorded at three different photon energies, 605, 620, and 650 eV. For comparison, a conventional uv photoelectron spectrum recorded at 60 eV photon energy is included. The latter has been shifted by about 560 eV in order to line up the first photoelectron band with the first peak of the double ionization spectrum.

The figure also includes a conventional uv photoelectron spectrum [14,29] recorded at 60 eV photon energy [29] which is known to reflect the lowest single ionization threshold at around 12.07 eV. It has been shifted by about 560 eV in order to line up the first photoelectron band with the first peak of the double ionization spectrum. The main features of this spectrum agree to a large extent with the features of the double ionization spectra, although with much narrower spectral lines. Thus, the energy shift of all valence orbitals due to the core vacancy in the dication seems to be of similar

TABLE I. Calculated double ionization energies of O_2 with the corresponding leading configurations and term symbols given in $D_{\infty h}$ symmetry.

Ionization potential (eV)	Leading configuration	Term symbol
570.225	$(1\sigma_g)^1\cdots(1\pi_u)^4(1\pi_g)^1$	$^1\Pi_g$
570.313	$(1\sigma_u)^1\cdots(1\pi_u)^4(1\pi_g)^1$	$^1\Pi_u$
577.286	$(1\sigma_g)^1\cdots(1\pi_u)^3(1\pi_g)^2$	$^1\Pi_u$
577.370	$(1\sigma_u)^1\cdots(1\pi_u)^3(1\pi_g)^2$	$^1\Pi_g$
577.920	$(1\sigma_g)^1\cdots(3\sigma_g)^1$	$^1\Sigma_g^-$
578.006	$(1\sigma_u)^1\cdots(3\sigma_g)^1$	$^1\Sigma_u^-$
569.665	$(1\sigma_g)^1\cdots(1\pi_u)^4(1\pi_g)^1$	$^3\Pi_g$
569.754	$(1\sigma_u)^1\cdots(1\pi_u)^4(1\pi_g)^1$	$^3\Pi_u$
576.170	$(1\sigma_g)^1\cdots(3\sigma_g)^1$	$^3\Sigma_g^-$
576.256	$(1\sigma_u)^1\cdots(3\sigma_g)^1$	$^3\Sigma_u^-$
576.269	$(1\sigma_g)^1\cdots(1\pi_u)^3(1\pi_g)^2$	$^3\Pi_u$
576.377	$(1\sigma_u)^1\cdots(1\pi_u)^3(1\pi_g)^2$	$^3\Pi_g$
576.443	$(1\sigma_g)^1\cdots(1\pi_u)^3(1\pi_g)^2$	$^3\Pi_u$
576.549	$(1\sigma_u)^1\cdots(1\pi_u)^3(1\pi_g)^2$	$^3\Pi_g$
573.206	$(1\sigma_g)^1\cdots(1\pi_u)^3(1\pi_g)^2$	$^5\Pi_u$
573.300	$(1\sigma_u)^1\cdots(1\pi_u)^3(1\pi_g)^2$	$^5\Pi_g$
574.456	$(1\sigma_g)^1\cdots(3\sigma_g)^1$	$^5\Sigma_g^-$
574.549	$(1\sigma_u)^1\cdots(3\sigma_g)^1$	$^5\Sigma_u^-$

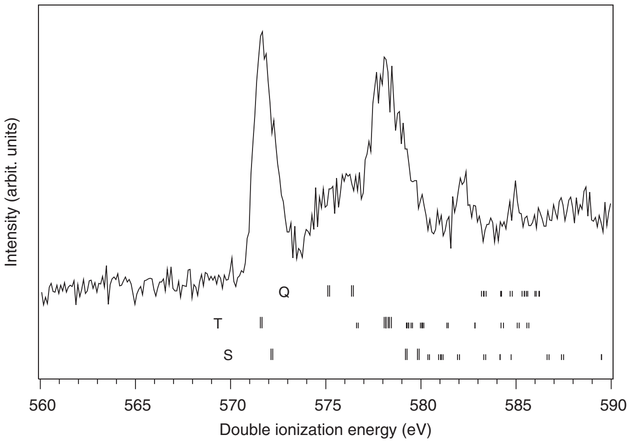

FIG. 2. An enlargement of the core-valence double ionization spectrum of molecular oxygen recorded at 620 eV. Calculated energies, arranged according to the multiplicity of the states (singlet, triplet, quintet), are included for comparison. The pure two-electron ejection states are shown by taller bars and those with additional excitations or spin flips with shorter bars. The calculated energies have been shifted by a constant value of 1.9 eV in order to emphasize the correspondence.

magnitude. This observation suggests that the core-valence interaction is principally of Coulombic origin, and that details of the hole-hole coupling, e.g., related to localization, are of secondary importance in this small molecule. Since the binding energy of the O 1*s* electron is approximately 544 eV [13] the core-valence interaction energy in molecular oxygen is of the order of 16 eV. To address details of the core-valence interaction we compare the experimental results with predictions based on *ab initio* calculations. Assignments of the double photoionization spectra will be proposed on the basis of the ground-state valence electron configuration given above and the calculated results given in Table I.

The calculations include singlet, triplet, and quintet states and should be complete up to at least 580.9 eV, whereas for higher energies some states of these multiplicities may be missing. For simplicity, only states whose leading configurations correspond to pure double ionization without any further excitations or spin flips are given in the table.

In order to provide a basis for more detailed assignments of the spectrum, Fig. 2 shows an enlargement of the spectrum obtained at a photon energy of 620 eV along with all the calculated double ionization energies (DIEs) up to around 590 eV. The pure doubly ionized states have been marked by longer bars and those with additional excitations or spin flips with shorter bars. The energies of the former states are given in Table I. Overall, there is a very good agreement between the experimentally observed peaks as listed in Table II and the calculated energies (cf. Table I), which gives support to the assignments. The calculated energies appear at about 1–2 eV lower ionization energies than the experimental values. This is likely to be due to a better description of the O_2^{2+} dication than of the O_2 neutral molecule, resulting from the additional number of electrons in O_2 that must be correlated. In Fig. 2 the theoretical results have been shifted by a constant value of 1.9 eV in order to emphasize the correspondence.

By comparison also with the uv photoelectron spectrum, the outermost band can be associated with a vacancy in the outermost valence orbital, $1\pi_g$, along with the O 1*s* vacancy. Two different molecular orbitals, $1\sigma_g$ and $1\sigma_u$, can be formed out of the O 1*s* orbitals, but the energy separation between them is too small (50 meV) [13] to be observed in the present spectra. The spins of the final states can be arranged to form one triplet and one singlet state, which together give rise to the peak. A doublet structure may be inferred in this peak corresponding to two overlapping lines at 571.6 and 572.3 eV, respectively (cf. Table II). This agrees very well with the calculated energy splitting of 0.6 eV, which gives support for the interpretation.

In the range between 574 and 577 eV some weaker features can be discerned. Again, the photoelectron spectrum is useful for the interpretation, which is made primarily in terms of a vacancy in the $1\pi_u$ orbital along with the O 1*s* vacancy. According to the calculations, the first structure, observed at 575.0 eV can be ascribed essentially to $^5\Pi$ states, whereas the next peak at 576.1 eV is a reflection of both $^5\Sigma$ and $^3\Pi$ states with nearly the same energy.

The next peak, located at around 578 eV, is very strong and broad, and is apparently due to a number of different dicationic states. The calculations suggest that both triplet and singlet states are present in this range, but with triplet states located primarily on the low ionization energy side and singlet states on the high ionization energy side, giving rise to the pronounced tail. This assignment, associating most of the intensity on the low binding energy side of the peak with $1\sigma_{g,u}^{-1}3\sigma_g^{-1}\ ^3\Sigma_{g,u}^-$ states agrees well with the location of the

TABLE II. Experimental double ionization energies and assignments of the O_2 core-valence double ionization spectrum.

Expt. DIEs (eV)	Assignment (leading configuration and term symbol)		Comment
571.6	$(1\sigma_{g,u})^1\cdots(1\pi_u)^4(1\pi_g)^1$	$^3\Pi_{g,u}$	Peak max
572.3	$(1\sigma_{g,u})^1\cdots(1\pi_u)^4(1\pi_g)^1$	$^1\Pi_{g,u}$	Shoulder
575.0	$(1\sigma_{g,u})^1\cdots(1\pi_u)^3(1\pi_g)^2$	$^5\Pi_{g,u}$	Peak max
576.1	$\begin{cases}(1\sigma_{g,u})^1\cdots(3\sigma_g)^1\\(1\sigma_{g,u})^1\cdots(1\pi_u)^3(1\pi_g)^2\end{cases}$	$^5\Sigma^-_{g,u}$ $^3\Pi_{g,u}$	Weak peak max
578.0	$\begin{cases}(1\sigma_{g,u})^1\cdots(3\sigma_g)^1\\(1\sigma_{g,u})^1\cdots(1\pi_u)^3(1\pi_g)^2\end{cases}$	$^3\Sigma^-_{g,u}$ $^3\Pi_{g,u}$	Peak max
579.5	$(1\sigma_{g,u})^1\cdots(3\sigma_g)^1$	$^1\Sigma_{g,u}$	Shoulder
579.5	$(1\sigma_{g,u})^1\cdots(1\pi_u)^3(1\pi_g)^2$	$^1\Pi_{g,u}$	Shoulder
580.8			Plateau
582.3			Peak max
585.0	$(1\sigma_{g,u})^1\cdots(3\sigma_g)^1$	$^5\Sigma^-_{g,u}$	Peak max

$b\,^4\Sigma^-_g$ state of the uv photoelectron spectrum (cf. Fig. 1). Another part of the intensity probably comes from singlet and triplet coupled O $1s^{-1}$ $1\pi_u^{-1}$ states as suggested by the calculations.

In the ordinary photoelectron spectrum the $3\sigma_g^{-1}$ ionization is reflected not only by the $b\,^4\Sigma^-_g$ state at 18.5 eV but also by the $B\,^2\Sigma^-_g$ state at 20.5 eV (see Ref. [14]). As suggested by the calculations, the $^1\Sigma^+_g$ states corresponding to the latter of these states may explain the plateau at around 581 eV.

Some further peaks can be discerned in the double ionization energy region above 581 eV. The two strongest of these peaks are observed at 582.3 and 585.0 eV. The first one has no direct correspondence with the uv photoelectron spectrum, whereas the second fits well with the $c\,^4\Sigma^-_u$ state of the cation. The calculations predict several quintet states of Σ symmetry in the energy region of the second peak, which agree well with the location of this $^4\Sigma^-_u$ state. It is expected that the $(1\sigma_{g,u})^{-1}\cdots(3\sigma_g)^{-1}$ configuration is important in the formation of these quintet states, and it is therefore given in Table II. For the peak at 582.3 eV, the calculations predict several singlet states of Π symmetry.

The spectra suggest several more electronic states above 586 eV (only partially shown in Figs. 1 and 2). However, since the calculations are incomplete in this energy range, we refrain from further detailed discussions.

Double ionization spectra in general (like the present ones, Auger or double charge transfer spectra) expose electronic states that are intrinsically more correlated than single ionization spectra. In fact, even for quite small first row molecules, there is a breakdown of the molecular orbital picture governing a large part of the spectra (especially inner-inner valence regions, but also large parts of the inner-outer valence regions). This is due to the fact that semi-internal excitations (external coupled to internal excitations) become energetically able to strongly interact with the main doubly ionized states, something that usually occurs only for the inner valence states in normal XPS [30,31]. The present spectra of molecular oxygen present an interesting variation on this since (i) the presence of an open shell increases the possibilities for semi-internal excitations [30], and therefore an increase of the breakdown effects, (ii) changing a valence to a core hole can be expected to reduce the breakdown effects. It is clear from the comparison with the normal UPS spectrum of O_2 (cf. Fig. 1), and from the weights of the leading coefficients in the CI expansion that the latter trend is the dominant one, thus that restoration of the one-particle picture is in some sense stronger than the breakdown effects induced by having an open shell already in the ground state.

The present core-valence spectra reflect in a very crude approximation the relative intensities from the uv photoelectron spectrum. This may suggest that the transition creating the valence hole is not strongly altered by the involvement of the O $1s$ core electron. It may be related to the fact that the kinetic energies of the outgoing valence electrons are of similar magnitude in the uv photoelectron spectrum and the core-valence spectra, but such an interpretation can be applied only if the double ionization is mainly direct. Indirect processes like autoionization from highly excited states of singly ionized molecules (e.g., $1s2s$ $2h$-$1p$ states) could be an additional supplier of intensity, but the relative amplitude of such processes tends to depend on the photon energy used. In the present study, the spectra obtained at different photon energies are very similar indeed to each other, which suggests that the intensity is acquired mainly via direct processes. The same conclusion is reached by examination of the electron energy distributions produced in formation of the principal bands in the spectra. The distributions appear monotonic, apart from spurious peaks at zero electron energy, which seem to arise from background interference.

V. SUMMARY

Core-valence double ionization spectra of molecular oxygen have been recorded at three different photon energies (605 eV, 620 eV, and 650 eV) using the TOF-PEPECO technique. The spectrum has been interpreted on the basis of results obtained from MCSCF calculations and in comparison with the ultraviolet photoelectron spectrum. There is an obvious similarity between the core-valence and the uv photoelectron spectrum, which suggests that the involvement of the core hole gives mainly rise to a Coulombic type of energy shift of the valence levels of the order of 16 eV. Structures in the core-valence spectrum are broad because of the large number of electronic states associated with different spin-spin couplings and with the gerade-ungerade splitting of the core levels, in addition to the short core-hole lifetime.

ACKNOWLEDGMENTS

This work has been financially supported by the Swedish Research Council (VR), the Göran Gustafsson Foundation (UU/KTH), the Knut and Alice Wallenberg Foundation, and the Wenner-Gren Foundation, Sweden. J.H.D.E. thanks the Leverhulme Trust for financial support. We are grateful to the technical support of the workshop staff at the AlbaNova Research Centre in Stockholm as well as at the Ångström Laboratory in Uppsala when adopting the experimental setup to synchrotron radiation. Furthermore, we would like to warmly acknowledge the support by the staff and colleagues at BESSY, Berlin. This work was also supported by the European Community - Research Infrastructure Action under the FP6 "Structuring the European Research Area" Programme (through the Integrated Infrastructure Initiative "Integrating Activity on Synchroton and Free Electron Laser Science" Contract No. R II 3-CT-2004-506008).

[1] J. H. D. Eland, O. Vieuxmaire, T. Kinugawa, P. Lablanquie, R. I. Hall, and F. Penent, Phys. Rev. Lett. **90**, 053003 (2003).
[2] F. Penent, J. Palaudoux, P. Lablanquie, L. Andric, R. Feifel, and J. H. D. Eland, Phys. Rev. Lett. **95**, 083002 (2005).
[3] P. Kruit and F. H. Read, J. Phys. E **16**, 313 (1983).
[4] J. H. D. Eland, S. S. W. Ho, and H. L. Worthington, Chem. Phys. **290**, 27 (2003).
[5] J. H. D. Eland, Chem. Phys. **294**, 171 (2003).
[6] J. H. D. Eland, R. Feifel, and D. Edvardsson, J. Phys. Chem. A **108**, 9721 (2004).
[7] A. Pilcher-Clayton and J. H. D. Eland, J. Electron Spectrosc. Relat. Phenom. **142**, 313 (2005).
[8] R. Feifel, J. H. D. Eland, and D. Edvardsson, J. Chem. Phys. **122**, 144308 (2005).
[9] R. Feifel, J. H. D. Eland, L. Storchi, and F. Tarantelli, J. Chem. Phys. **122**, 144309 (2005).
[10] R. D. Molloy, A. Danielsson, L. Karlsson, and J. H. D. Eland, Chem. Phys. **335**, 35 (2007).
[11] Y. Hikosaka, T. Aoto, P. Lablanquie, F. Penent, E. Shigemasa, and K. Ito, Phys. Rev. Lett. **97**, 053003 (2006).
[12] Y. Hikosaka, T. Kaneyasu, E. Shigemasa, P. Lablanquie, F. Penent, and K. Ito, J. Chem. Phys. **127**, 044305 (2007).
[13] S. Sorensen, K. J. Borve, R. Feifel, K. Ueda, and A. de Fanis, J. Phys. B **41**, 095101 (2008).
[14] P. Baltzer, B. Wannberg, L. Karlsson, M. Carlsson Göthe, and M. Larsson, Phys. Rev. A **45**, 4374 (1992).
[15] M. Larsson, P. Baltzer, S. Svensson, B. Wannberg, N. Mårtensson, A. Naves de Brito, N. Corriea, M. P. Keane, M. Carlsson Göthe, and L. Karlsson, J. Phys. B **23**, 1175 (1990).
[16] S. L. Sorensen, T. Tanaka, R. Feifel, J. H. D. Eland, M. Kitajima, H. Tanaka, R. Sankari, A. De Fanis, M.-N. Piancastelli, L. Karlsson, and K. Ueda, Chem. Phys. Lett. **398**, 168 (2004).
[17] P. Bolognesi, D. B. Thompson, L. Avaldi, M. A. MacDonald, M. C. A. Lopes, D. R. Copper, and G. C. King, Phys. Rev. Lett. **82**, 2075 (1999).
[18] J. H. D. Eland, and R. Feifel, Chem. Phys. **327**, 85 (2006).
[19] K. J. S. Sawhney, F. Senf, and W. Gudat, Nucl. Instrum. Methods Phys. Res. A **467-468**, 466 (2001).
[20] D. R. Batchelor, R. Follath, and D. Schmeisser, Nucl. Instrum. Methods Phys. Res. A **467**, 470 (2001).
[21] http://www.bessy.de/
[22] A. A. Cafolla, T. Reddish, and J. Comer, J. Phys. B **22**, L273 (1989).
[23] Dalton, a molecular electronic structure program, Release 2.0, 2005, see http://www.kjemi.uio.no/software/dalton/dalton.html
[24] T. H. Dunning, Jr., J. Chem. Phys. **90**, 1007 (1989).
[25] R. A. Kendall, T. H. Dunning, Jr., and R. J. Harrison, J. Chem. Phys. **96**, 6796 (1992).
[26] P. S. Bagus and H. F. Schaefer III, J. Chem. Phys. **56**, 224 (1972).
[27] H. Ågren, P. S. Bagus, and B. O. Roos, Chem. Phys. Lett. **82**, 505 (1981).
[28] E. Tiemann, J. Mol. Spectrosc. **91**, 60 (1982).
[29] R. Feifel *et al.* (unpublished).
[30] H. Ågren, J. Chem. Phys. **75**, 1267 (1981).
[31] H. Ågren, A. Cesar, and C. M. Liegener, Adv. Quantum Chem. **23**, 1 (1992).